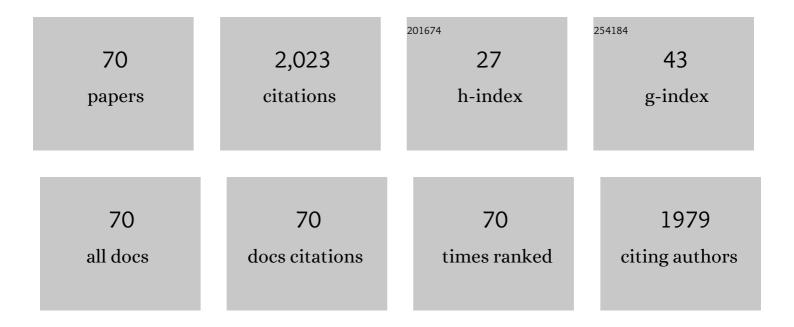
List of Publications by Year in descending order

Source: https://exaly.com/author-pdf/8060565/publications.pdf Version: 2024-02-01



**ΥΠΝΕΙΙ ΡΑΝ** 

#	Article	IF	CITATIONS
1	A fully integrated graphene-polymer field-effect transistor biosensing device for on-site detection of glucose in human urine. Materials Today Chemistry, 2022, 23, 100635.	3.5	8
2	An Ultraflexible and Transparent Grapheneâ€Based Wearable Sensor for Biofluid Biomarkers Detection. Advanced Materials Technologies, 2022, 7, .	5.8	9
3	Ultrasensitive Graphene-Based Nanobiosensor for Rapid Detection of Hemoglobin in Undiluted Biofluids. ACS Applied Bio Materials, 2022, 5, 1624-1632.	4.6	2
4	Ultra-sensitive and rapid screening of acute myocardial infarction using 3D-affinity graphene biosensor. Cell Reports Physical Science, 2022, 3, 100855.	5.6	17
5	Eco-friendly Dopamine-Modified Silica Nanoparticles for Oil-Repellent Coatings: Implications for Underwater Self-Cleaning and Antifogging Applications. ACS Applied Nano Materials, 2022, 5, 8038-8047.	5.0	11
6	A Flexible and Regenerative Aptameric Graphene–Nafion Biosensor for Cytokine Storm Biomarker Monitoring in Undiluted Biofluids toward Wearable Applications. Advanced Functional Materials, 2021, 31, 2005958.	14.9	86
7	Cytokine Storm Biomarkers: A Flexible and Regenerative Aptameric Graphene–Nafion Biosensor for Cytokine Storm Biomarker Monitoring in Undiluted Biofluids toward Wearable Applications (Adv.) Tj ETQq1 1 C	).78 <b>43.</b> 04 rg	gBT1/Overlock
8	An Intelligent Grapheneâ€Based Biosensing Device for Cytokine Storm Syndrome Biomarkers Detection in Human Biofluids. Small, 2021, 17, e2101508.	10.0	44
9	Ultra-robust superwetting hierarchical membranes constructed by coordination complex networks for oily water treatment. Journal of Membrane Science, 2021, 627, 119234.	8.2	79
10	Hygro-responsive, Photo-decomposed Superoleophobic/Superhydrophilic Coating for On-Demand Oil–Water Separation. ACS Applied Materials & Interfaces, 2021, 13, 35142-35152.	8.0	46
11	Core-shell magnetic nanoparticles for substrate-Independent super-amphiphobic surfaces and mechanochemically robust liquid marbles. Chemical Engineering Journal, 2020, 391, 123523.	12.7	20
12	A Wearable and Deformable Graphene-Based Affinity Nanosensor for Monitoring of Cytokines in Biofluids. Nanomaterials, 2020, 10, 1503.	4.1	43
13	Superhydrophilic Al <sub>2</sub> O <sub>3</sub> Particle Layer for Efficient Separation of Oil-in-Water (O/W) and Water-in-Oil (W/O) Emulsions. Langmuir, 2020, 36, 13285-13291.	3.5	14
14	Modulating the Linker Immobilization Density on Aptameric Graphene Field Effect Transistors Using an Electric Field. ACS Sensors, 2020, 5, 2503-2513.	7.8	40
15	Multifunctional TiO <sub>2</sub> -Based Superoleophobic/Superhydrophilic Coating for Oil–Water Separation and Oil Purification. ACS Applied Materials & Interfaces, 2020, 12, 18074-18083.	8.0	87
16	An integrated flexible and reusable graphene field effect transistor nanosensor for monitoring glucose. Journal of Materiomics, 2020, 6, 308-314.	5.7	26
17	Slip-shear and inertial migration of finite-size spheres in plane Poiseuille flow. Computational Materials Science, 2020, 176, 109542.	3.0	1
18	ANALYSIS OF LIQUID MEDIATED CONTACT OF GLASS COLLOIDAL PARTICLE WITH POLYSTYRENE COATED SURFACE. Surface Review and Letters, 2020, 27, 1950101.	1.1	0

#	Article	lF	CITATIONS
19	On-demand oil/water separation enabled by magnetic super-oleophobic/super-hydrophilic surfaces with solvent-responsive wettability transition. Applied Surface Science, 2020, 533, 147092.	6.1	27
20	Sensitive detection of lung cancer biomarkers using an aptameric graphene-based nanosensor with enhanced stability. Biomedical Microdevices, 2019, 21, 65.	2.8	29
21	Surfaces with controllable super-wettability and applications for smart oil-water separation. Chemical Engineering Journal, 2019, 378, 122178.	12.7	52
22	Ultraviolet-driven switchable superliquiphobic/superliquiphilic coating for separation of oil-water mixtures and emulsions and water purification. Journal of Colloid and Interface Science, 2019, 557, 395-407.	9.4	48
23	Establishment of a Standard Method for Boundary Slip Measurement on Smooth Surfaces Based on AFM. Applied Sciences (Switzerland), 2019, 9, 1453.	2.5	7
24	Rapid, ultraviolet-induced, reversibly switchable wettability of superhydrophobic/superhydrophilic surfaces. Beilstein Journal of Nanotechnology, 2019, 10, 866-873.	2.8	23
25	Bioinspired superoleophobic/superhydrophilic functionalized cotton for efficient separation of immiscible oil-water mixtures and oil-water emulsions. Journal of Colloid and Interface Science, 2019, 548, 123-130.	9.4	109
26	Graphene-based fully integrated portable nanosensing system for on-line detection of cytokine biomarkers in saliva. Biosensors and Bioelectronics, 2019, 134, 16-23.	10.1	115
27	Mechanochemical robust, magnetic-driven, superhydrophobic 3D porous materials for contaminated oil recovery. Journal of Colloid and Interface Science, 2019, 538, 25-33.	9.4	37
28	Flexible, Durable, and Unconditioned Superoleophobic/Superhydrophilic Surfaces for Controllable Transport and Oil–Water Separation. Advanced Functional Materials, 2018, 28, 1706867.	14.9	203
29	Size dependences of hydraulic resistance and heat transfer of fluid flow in elliptical microchannel heat sinks with boundary slip. International Journal of Heat and Mass Transfer, 2018, 119, 647-653.	4.8	43
30	Preparation of colloidal crystal template for inverse opal hydrogels. Composite Interfaces, 2018, 25, 251-258.	2.3	1
31	Measurement of cytokine biomarkers using an aptamer-based affinity graphene nanosensor on a flexible substrate toward wearable applications. Nanoscale, 2018, 10, 21681-21688.	5.6	69
32	Selective Superwettability: Flexible, Durable, and Unconditioned Superoleophobic/Superhydrophilic Surfaces for Controllable Transport and Oil–Water Separation (Adv. Funct. Mater. 20/2018). Advanced Functional Materials, 2018, 28, 1870136.	14.9	3
33	Measurement and Quantification of Effective Slip Length at Solid–Liquid Interface of Roughness-Induced Surfaces with Oleophobicity. Applied Sciences (Switzerland), 2018, 8, 931.	2.5	9
34	Effective Boundary Slip Induced by Surface Roughness and Their Coupled Effect on Convective Heat Transfer of Liquid Flow. Entropy, 2018, 20, 334.	2.2	8
35	Humanoid Identification of Fabric Material Properties by Vibration Spectrum Analysis. Sensors, 2018, 18, 1820.	3.8	4
36	Characterization and Bioreplication of <i>Tradescantia pallida</i> Inspired Biomimetic Superwettability for Dual Way Patterned Water Harvesting. Advanced Materials Interfaces, 2018, 5, 1800723.	3.7	14

#	Article	IF	CITATIONS
37	Valid data based normalized cross-correlation (VDNCC) for topography identification. Neurocomputing, 2018, 308, 184-193.	5.9	37
38	Optimal fractal tree-like microchannel networks with slip for laminar-flow-modified Murray's law. Beilstein Journal of Nanotechnology, 2018, 9, 482-489.	2.8	17
39	Coexistence of superhydrophilicity and superoleophobicity: theory, experiments and applications in oil/water separation. Journal of Materials Chemistry A, 2018, 6, 15057-15063.	10.3	102
40	Joule heating, viscous dissipation and convective heat transfer of pressure-driven flow in a microchannel with surface charge-dependent slip. International Journal of Heat and Mass Transfer, 2017, 108, 1305-1313.	4.8	42
41	Effect of Surface Charge on the Nanofriction and Its Velocity Dependence in an Electrolyte Based on Lateral Force Microscopy. Langmuir, 2017, 33, 1792-1798.	3.5	7
42	The non-monotonic overlapping EDL-induced electroviscous effect with surface charge-dependent slip and its size dependence. International Journal of Heat and Mass Transfer, 2017, 113, 32-39.	4.8	28
43	Effect of surface morphology on measurement and interpretation of boundary slip on superhydrophobic surfaces. Surface and Interface Analysis, 2017, 49, 594-598.	1.8	10
44	A Facile and Effective Method to Fabricate Superhydrophobic/Superoeophilic Surface for the Separation of Both Water/Oil Mixtures and Water-in-Oil Emulsions. Polymers, 2017, 9, 563.	4.5	14
45	Tactile Perception of Roughness and Hardness to Discriminate Materials by Friction-Induced Vibration. Sensors, 2017, 17, 2748.	3.8	32
46	The effect of the electrical double layer on hydrodynamic lubrication: a non-monotonic trend with increasing zeta potential. Beilstein Journal of Nanotechnology, 2017, 8, 1515-1522.	2.8	8
47	Interface conditions of roughness-induced superoleophilic and superoleophobic surfaces immersed in hexadecane and ethylene glycol. Beilstein Journal of Nanotechnology, 2017, 8, 2504-2514.	2.8	2
48	Effect of Surface Roughness on the Measurement of Boundary Slip Based on Atomic Force Microscope. Science of Advanced Materials, 2017, 9, 122-127.	0.7	6
49	AFM Study on the Boundary Condition, Surface Potential and the Viscosity of the Magnetic Treated Liquids. Science of Advanced Materials, 2017, 9, 144-150.	0.7	2
50	Characterization of spherical domains at the polystyrene thin film–water interface. Beilstein Journal of Nanotechnology, 2016, 7, 581-590.	2.8	5
51	Simulation of Effective Slip and Drag in Pressure-Driven Flow on Superhydrophobic Surfaces. Journal of Nanomaterials, 2016, 2016, 1-9.	2.7	5
52	Study on Nanobubble-on-Pancake Objects Forming at Polystyrene/Water Interface. Langmuir, 2016, 32, 11256-11264.	3.5	19
53	Measurements of slip length for flows over graphite surface with gas domains. Applied Physics Letters, 2016, 109, .	3.3	12
54	Extraction of individual characteristics of breech face impressions in ballistic identification using optimal Gaussian filter parameters. , 2016, , .		0

#	Article	lF	CITATIONS
55	Study of the Relationship between Boundary Slip and Nanobubbles on a Smooth Hydrophobic Surface. Langmuir, 2016, 32, 11287-11294.	3.5	35
56	Electroviscous effect and convective heat transfer of pressure-driven flow through microtubes with surface charge-dependent slip. International Journal of Heat and Mass Transfer, 2016, 101, 648-655.	4.8	45
57	Surface charge-induced EDL interaction on the contact angle of surface nanobubbles. Langmuir, 2016, 32, 11123-11132.	3.5	10
58	Atomic Force Microscopy Measurement of Slip on Smooth Hydrophobic Surfaces and Possible Artifacts. Journal of Physical Chemistry C, 2015, 119, 12531-12537.	3.1	13
59	Design and analysis of a GMM actuator for active vibration isolation. , 2015, , .		0
60	The study of surface wetting, nanobubbles and boundary slip with an applied voltage: A review. Beilstein Journal of Nanotechnology, 2014, 5, 1042-1065.	2.8	48
61	Analysis of Slip Induced One Dimensional MHD Flow between Parallel Plates. Applied Mechanics and Materials, 2014, 618, 159-163.	0.2	0
62	Coalescence and Stability Analysis of Surface Nanobubbles on the Polystyrene/Water Interface. Langmuir, 2014, 30, 6079-6088.	3.5	47
63	Influence of Polystyrene (PS) solution concentration on the formation of nanobubbles. , 2013, , .		1
64	Role of surface charge on boundary slip in fluid flow. Journal of Colloid and Interface Science, 2013, 392, 117-121.	9.4	37
65	AFM characterization of nanobubble formation and slip condition in oxygenated and electrokinetically altered fluids. Journal of Colloid and Interface Science, 2013, 392, 105-116.	9.4	39
66	Slip Length Measurement of Confined Air Flow on Three Smooth Surfaces. Langmuir, 2013, 29, 4298-4302.	3.5	5
67	An improved method for measuring boundary slip on hydrophobic surface with atomic force microscope. , 2013, , .		0
68	Hydrodynamic drag-force measurement and slip length on microstructured surfaces. Physical Review E, 2012, 85, 066310.	2.1	33
69	Role of Electric Field on Surface Wetting of Polystyrene Surface. Langmuir, 2011, 27, 9425-9429.	3.5	27
70	Role of Electric Field on Electroviscosity. Advanced Materials Research, 0, 803, 438-441.	0.3	0